Journal of Materials and Environmental Sciences
ISSN : 2028-2508
CODEN : JMESCN

J. Mater. Environ. Sci., 2019, Volume 10, Issue 9, Page 854-871

http://www.jmaterenvironsci.com

Structural Studies and Spectroscopic properties of Quinolizidine Alkaloids (+) and (-)-Lupinine in different media

José Ruiz Hidalgo, Maximiliano A. Iramain, Silvia Antonia Brandán*

Cátedra de Química General, Instituto de Química Inorgánica, Facultad de Bioquímica. Química y Farmacia, Universidad Nacional de Tucumán, Ayacucho 471, (4000) San Miguel de Tucumán, Tucumán, Argentina.

Received 21 Aug 2019,
Revised 07 Sept 2019,
Accepted 09 Sept 2019

Keywords
- ✓ (-)-Lupinine,
- ✓ Structural properties,
- ✓ Force fields,
- ✓ Vibrational analysis,
- ✓ DFT calculations.

**sbrandan@fbqf.unt.edu.ar*
Phone: +54-381-4247752;
Fax: +54-381-4248169

Abstract

The quinolizidine alkaloids, as numerous species of lupine (*Lupinus* spp.), are toxic and have biological effect on the nervous system. Hence, four (+) and (-)- molecular structures of quinolizidine alkaloid lupinine, named C0, C1a, C1b and C1c have been theoretically determined in gas phase and in aqueous solution by using hybrid B3LYP/6-31G* calculations. The studied properties have evidenced that the most stable C1c form present the higher populations in both media while the predicted infrared, Raman, ^{1}H-NMR and ^{13}C-NMR and ultra-visible spectra suggest that probably other forms in lower proportion could be also present in water, chloroform and benzene solutions, as evidenced by the low RMSD values observed in the ^{1}H- and ^{13}C-NMR chemical shifts. The C1c form presents the lower corrected solvation energy in water while the NBO and AIM studies suggest for this form a high stability in both media. In addition, the predicted ECD spectra of all (+) and (-)-lupinine forms in methanol solution evidence clearly that the C1b forms is present in the solution because its spectrum presents a negative Cotton effect as observed in the experimental one.

1. Introduction

Alkaloids are compounds very interesting from different points of view because they present a wide range of pharmacological properties, for which, these species are highly used in therapy medicinal to control the pain while also present several side effects mainly as abuse drugs [1,2]. Recent structural studies on tropane alkaloids such as scopolamine, morphine, heroin, cocaine and tropane have evidenced interesting correlations among the properties of free base, cationic and hydrochloride species derived from these alkaloids [3-7].

Other species with different rings in its structures, such as indol alkaloid, specifically N-(1H-indol-3-ylmethyl)-N,N-dimethylamine, named gramine or the 4-bromo-2,5-dimethoxyphenethylamine derivative, known as 2C-B, also present similar biological activities despite of their clear structural differences [8,9]. In this work, we have studied the different configurations and structures of alkaloid (+) and (-)-lupinine together with their vibrational properties. These studies are important taking into account that numerous species of lupine (*Lupinus* spp.) are toxic and have biological effect on the nervous system. So far, these properties are not reported yet. The (+) and (-)-lupinine structures present a tertiary N atom in the quinozilidine rings with a hydroxyl group in *Trans* position in relation to ring. Previously, the absolute configurations of lupinine and its chemistry and physiology properties were studied [10-14] and then, the structure of this alkaloid was experimentally determined by X-ray diffraction by Koziol et al [15]. Both rings belonging to quinozilidine present chairs conformations, as in the tropane rings and their properties are known form long time [16-35]. Those authors have suggested that the OH group presents intra-molecular hydrogen bonds which could explain the broad band observed in the IR spectrum at 3170 cm^{-1} and, this way, they have not confirmed but have suggested that further spectroscopic investigations are necessary to explain the nature of the hydrogen bond in solution.

On the other hand, the IR spectrum of lupinine was recorded in the 1951 year but the spectrum in that opportunity was not presented and only the band at 3400 cm^{-1} was assigned to OH stretching mode [16]. Posteriors studies on the IR spectrum of lupinine were later reported, in one of them the authors have found a correlation

between the stereochemistry of quinolizidine alkaloids and the IR spectra in the 2862-2600 cm^{-1} region [18] and, in the most recent work, only four bands of IR spectrum at 3419, 3389, 2820 and 1406 were identified and assigned [27]. Additional spectroscopic studies of lupinine based on ^{1}H- and ^{13}C-NMR [19-21,23], UV-visible [17,35] and Electronic Circular Dichroism (ECD) spectra [35] were also reported. Obviously, the theoretical structural studies on all possible configurations of lupinine are very important to elucidate the existence of an intra-molecular H bond with the structural requirement of the N---O distance should be about 2.6 Å, as was experimentally suggested by Koziol et al [15]. Hence, the aims of this work are: (i) to study all theoretical structures of chair conformations of (+) and (-)-lupinine in gas phase and in aqueous and in methanol solutions by using the hybrid B3LYP/6-31G* method [36,37], (ii) to study atomic charges, solvation and stabilization energies, molecular electrostatic potentials and topological properties at the same level of theory, (iii) to predict the reactivities and behaviours of those structures in both media by using the frontier orbitals and equations before reported [41-45] and finally, (iv) to perform the complete vibrational assignments of (+) and (-)-lupinine structures by using the scaled quantum mechanical force field (SQMFF) approach and the Molvib program. Here, the normal internal coordinates, infrared and Raman spectra and force fields of (+) and (-)-lupinine structures were predicted and compared with those published in the literature [27]. Additionally, the ^{1}H- and ^{13}C-NMR, Ultraviolet-visible and ECD spectra of both structures of lupinine were also predicted at the same level of theory and, later, compared with the corresponding experimental ones.

2. Material and Methods

The (+) and (-)-lupinine structures, named C0, C1a, C1b and C1c in accordance to the structures proposed by Halpern and Legenza [22] were modelled with the *GaussView* program [46] and, later these structures were optimized in gas phase and in aqueous and methanol solution with the Revision A.02 of Gaussian program [47] and the hybrid B3LYP/6-31G* method [36,37]. The (+)-lupinine structure corresponds to C0 while the other ones correspond to (-)-lupinine structures. All structures present chair conformations but C1c differ from the other ones in the position of OH group. In **Figure 1** are given all conformations together with the atoms labelling and the identification of the two rings while **Figure 2** shows clearly the different positions that adopt the OH groups in C1b and C1c. Thus, in C0, C1a and C1b, the OH group is oriented out-of-rings while in C1c the group is oriented towards the rings forming with the N2 atom an H bond of type O1-H31---N2.

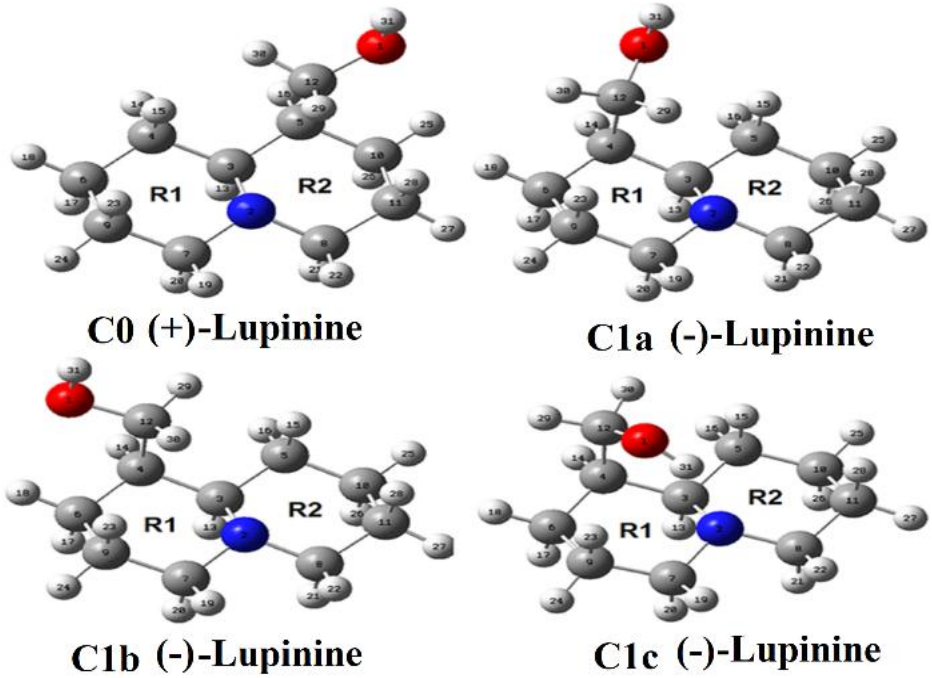

Figure 1: Molecular theoretical structures of all (+) and (-)-Lupinine forms, atoms labelling and identifications of their rings

The solvent effects were studied with the integral equation formalism variant polarised continuum method (IEFPCM) while the solvation energies were predicted for with the universal solvation model [48-50]. The solvation energies were corrected by zero point vibrational energy (ZPVE) and by non-electrostatic terms while the volumes of all conformations were computed with the Moldraw program [51].

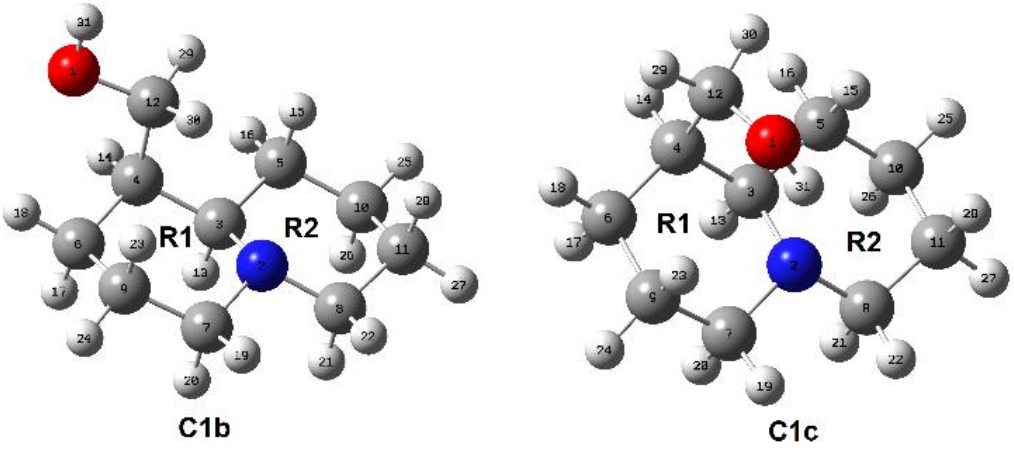

Figure 2 : Molecular theoretical C1b and C1c structures of (-)-Lupinine showing the same chairs conformations and the different positions of OH groups.

The NBO and AIM2000 programs [52-54] and Merz-Kollman (MK) charges [55] were employed to calculate atomic charges, bond orders, molecular electrostatic potentials, stabilization energies, and topological properties at the same level of theory. The frontier orbitals and the gap calculations were used to predict the reactivities of all structures, as suggested by Parr and Pearson [56] while their behaviours in both media were predicted at the same level of theory by using known descriptors [41-45,57]. The harmonic force fields and force constants were calculated by using the transferable scale factors, the normal internal coordinates with the scaled quantum mechanical force field (SQMFF) methodology and the Molvib program [38-40]. Here, energy distribution (PED) contributions ≥ 10% were used to perform the complete vibrational assignments. The Raman spectra predicted in activities were changed to intensities to obtain a better correlation by using recognized equations [58,59]. The ^{1}H- and ^{13}C-NMR spectra for all structures of lupinine were predicted by using the Gauge-Independent Atomic Orbital (GIAO) method [60] considering to Trimethylsilane (TMS) as reference. Additionally, the ultraviolet-visible and ECD spectra of all structures of lupinine were predicted with Time-dependent DFT calculations (TD-DFT) by using the same level of theory and the Gaussian 09 program [47]. Here, the predicted properties and the predicted spectraonly were compared for the most stable structures according to the suggested by Halpern and Legenza [22].

3. Results and discussion

Structures in both media

Calculated total uncorrected and corrected by zero point vibrational energy (ZPVE) energies, dipole moments and volumes and their variations for the four structures of lupinine in gas phase and in aqueous solution by using the B3LYP/6-31G* method are summarized in **Table 1**.

Table 1. Calculated total energies (*E*), dipole moments (μ) and volumes (V) of different configurations (+) and (-)- lupinine in gas phase and in aqueous solution.

B3LYP/6-31G* Method[a]					
Medium	E (Hartrees)	E ZPVE	μ (D)	V (Å^3)	ΔE(kJ/mol)
(+) Lupinine C0					
GAS	-522.4711	-522.1843	1.23	203.7	17.05
PCM/Water	-522.4820	-522.1954	1.58	201.9	8.66
(-) Lupinine C1a (2%)[#]					
GAS	-522.4710	-522.1844	1.14	203.5	16.79
PCM/Water	-522.4814	-522.1952	1.58	202.8	9.18
(-) Lupinine C1b (9%)[#]					
GAS	-522.4711	-522.1843	1.23	203.0	17.05
PCM/Water	-522.4820	-522.1954	1.58	203.7	8.66
(-) Lupinine C1c (89%)[#]					
GAS	-522.4788	-522.1908	2.76	201.3	0.00
PCM/Water	-522.4860	-522.1987	4.21	200.9	0.00

[a] This work, [#]Populations suggested by Halpern and Legenza [22]

The results of Table 1 shows that both total energy values uncorrected and corrected by ZPVE for the C1c form in the two media have lower values than the other ones, this way, C1c is clearly the most stable than C0, C1a and C1b, as suggested by Halpern and Legenza [22] and as revealed by the calculations performed here. According the studies of Halpern and Legenza [22] the population's % for C1a, C1b and C1c are 2, 9 and 89 %, respectively as indicated in Table 1. Here, our calculations predict that the populations of C1c in both media are approximately 99.70 % indicating the presence only of this conformer in both media. Probably, the higher dipole moment values observed for C1c in both media justify these observations, as was also observed in other species [8,9,61].
All conformations show increase in the dipole moments values in solution but C1b presents volume expansion in this medium while slight contraction volumes are observed in the other ones. Here, the dissimilar positions of OH groups in the structures could explain the difference in the volumes and their variations in solution because the water molecules hydrate in different form both structures. In C0, C1a and C1b, the hydrated OH groups have greater freedom of movement while in the C1c conformation the group is more restricted due to the presence of the hydrogen bond OH---N.

Corrected and uncorrected solvation energies by the total non-electrostatic terms and by zero point vibrational energy (ZPVE) for all forms of lupinine by using the B3LYP/6-31G* method can be seen in **Table 2**. The higher solvation energy value observed for C1a can be easily explained by the position of OH group and a greater freedom of movement of this group in this conformation which allows to it a higher hydration while in the C1c conformation the group is most restricted and, obviously less hydrated, as a consequence of H bond that form the OH group with the N atom. Hence, lower solvation energy value presents C1c.

Table 2. Corrected and uncorrected solvation energies by the total non-electrostatic terms and by zero point vibrational energy (ZPVE) of lupinine in gas phase and in aqueous solution together with their volume variations by using the B3LYP/6-31G* method.

B3LYP/6-31G* method[a]				
Solvation energy (kJ/mol)				ΔV (Å^3)
Medium	$\Delta G_{un}^{\#}$	ΔG_{ne}	ΔG_c	
		C0		
PCM/Water	-29.09	6.73	-35.82	-1.8
		C1a		
PCM/Water	-28.32	7.52	-35.84	-0.7
		C1b		
PCM/Water	-29.09	5,64	-34.73	0.7
		C1c		
PCM/Water	-20.73	11,57	-32.30	-0.4

[a]This work

$\Delta G_{un}^{\#}$= uncorrected solvation energy, ΔG_{ne}= total non-electrostatic terms, ΔG_c= corrected solvation energies.

Taking into account that all conformations of lupinine are weak bases their corresponding solvation energy values in aqueous solution were compared in **Table 3** with the values reported for the free bases of scopolamine, morphine, heroin, cocaine and tropane alkaloids [3-5,9,64], cyclizine, promethazine (PTZ) [61,62] and 2C-B [8].

The comparisons show that the different forms of lupinine have practically the same corrected solvation energies than gramine (-34.89 kJ/mol) and the S(-) form of PTZ (-36.07 kJ/mol) while the free base of heroin presents the most negative value (-88.67 kJ/mol) and, for this reason, it species has probably the higher solubility in water. The low ΔG_c values of all free bases, as compared with the cationic species of gramine (-261.58 kJ/mol) or cocaine (-255.24 kJ/mol), justify the use of the cationic or hydrochloride species in pharmaceutical preparations [5,9].

Geometries of all species in both media

The structure of the alkaloid lupinine was experimentally determined by X-ray diffraction by Koziol et al [15], hence, these values were compared in **Table 4** with those theoretical corresponding for the two species most stable of (-)-lupinine, C1b and C1c in gas phase and in aqueous solucion by using the hybrid B3LYP/6-31G* method. The variations between experimental and theoretical values were evaluated by means of the root-mean-square deviation (RMSD) values.

Table 3. Corrected solvation energies by the total non-electrostatic terms and by zero point vibrational energy (ZPVE) of lupinine in aqueous solution compared with other species by using the same method.

B3LYP/6-31G* method	
ΔG_c, Solvation energy (kJ/mol)	
Species	Free base
(+)-Lupinine C0[a]	-35.82
(-)-Lupinine C1a[a]	-35.84
(-)-Lupinine C1b[a]	-34.73
(-)-Lupinine C1c[a]	-32.30
Gramine[b]	-34.89
2C-B[c]	-49.31
S(-)-Promethazine[d]	-36.07
R(+)-Promethazine[d]	-17.87
Cyclizine[e]	-29.53
Morphine[f]	-60.91
Cocaine[g]	-71.26
Scopolamine[h]	-75.47
Heroin[i]	-88.67
Tropane[d]	-12.55

[a]This work, [b]From Ref [9], [c]From Ref [8], [d]From Ref [61], [e]From Ref [62], [f]From Ref [3], [g]From Ref [5], [h]From Ref [64], [i]From Ref [4,61]

Table 4. Comparison of calculated geometrical parameters for the two most stable species of (-)-lupinine in gas phase and in aqueous solution with the corresponding experimental ones.

B3LYP/6-31G* Method[a]					
Parameters	C1b		C1c		Experimental [b]
	Gas	Water	Gas	Water	
Bond lengths (Å)					
O1-C12	1.428	1.438	1.420	1.435	1.424
C12-C4	1.536	1.534	1.544	1.539	1.534
C4-C6	1.539	1.541	1.540	1.540	1.533
C6-C9	1.531	1.531	1.533	1.532	1.514
C9-C7	1.527	1.525	1.528	1.526	1.503
C7-N2	1.468	1.472	1.475	1.479	1.472
N2-C3	1.478	1.484	1.487	1.494	1.474
C3-C4	1.551	1.552	1.552	1.551	1.536
N2-C8	1.467	1.473	1.472	1.478	1.481
C8-C11	1.528	1.527	1.526	1.525	1.518
C11-C10	1.531	1.531	1.531	1.530	1.502
C10-C5	1.531	1.531	1.531	1.531	1.509
C5-C3	1.539	1.538	1.538	1.537	1.529
O1-H31	0.968	0.971	0.981	0.986	0.980
RMSD[b]	**0.015**	**0.015**	**0.015**	**0.015**	
Bond angles (º)					
H31-O1-C12	107.5	106.8	106.4	105.4	109
O1-C12-C4	108.2	107.8	114.8	114.3	109.3
C12-C4-C6	111.8	111.9	113.1	113.3	111.7
C12-C4-C3	112.9	114.9	113.0	112.9	112.4

C4-C6-C9	110.8	111.1	111.5	111.9	110.7
C6-C9-C7	110.3	110.2	110.2	110.3	109.8
C6-C4-C3	109.9	110.0	109.8	110.1	110.4
C9-C7-N2	112.7	112.6	112.8	112.7	112.7
C7-N2-C3	112.3	111.0	111.3	110.5	110.5
C7-N2-C8	108.7	107.9	108.6	108.0	108.3
N2-C3-C4	111.1	112.6	109.8	110.0	111.7
N2-C3-C5	110.7	110.5	110.7	110.6	109.7
N2-C8-C11	112.9	113.2	112.9	113.1	112.3
C8-N2-C3	112.3	110.6	112.3	111.2	110.4
C8-C11-C10	110.0	110.3	110.1	110.2	110.6
C11-C10-C5	109.0	109.2	109.1	109.3	110.2
C10-C5-C3	112.2	111.8	112.4	112.2	112.5
C5-C3-C4	112.5	112.8	112.3	112.4	112.9
RMSD[b]	**0.9**	**1.0**	**1.6**	**1.6**	
			Dihedral angles (º)		
O1- C12-C4-C3	-175.4	171.4	-54.9	-52.3	174.8
O1- C12-C4-C6	-50.9	-62.3	70.7	73.8	50
N2-C3-C4-C6	-55.9	-53.9	-57.5	-56.9	54.6
C7-N2-C3-C4	57.1	56.1	59.5	59.9	-56.5
C6-C9-C7-N2	54.9	57.0	54.1	54.6	-58.0
RMSD[b]	**184.7**	**100.2**	**135.4**	**134.7**	

[a]This work, [b]Ref [15]

Good correlations are observed in the RMSD values of bond lengths (0.015 Å) and angles (1.6-0.9 º) while the dihedral angles show the higher variations (184.7-100.2 º) where C1b in aqueous solution present the lower value (100.2 º). Note that C1c in both media present the dihedral O1-C12-C4-C6 angles with positive signs while in C1b the values are negative due to the different positions of OH groups in both conformations. The signs of other four dihedral angles are predicted different from the experimental ones, hence, the great difference observed in the RMSD values. Evidently, due to the good correlations observed in bond lengths and angles for C1c, it structures can clearly be used to perform the vibrational studies.

Atomic charges, molecular electrostatic potentials and bond orders studies

It is very important for the two most stable forms of lupinine in both media to analyse if the atomic charges, molecular electrostatic potentials and bond orders are affected by the change of orientation of OH group. Thus, three types of atomic charges were studied by using the B3LYP/6-31G* method which are Merz-Kollman (MK), Mulliken and natural population (NPA) charges. Molecular electrostatic potentials and bond orders studies were also calculated for C1b and C1c.

Thus, the different charges are presented in **Table S1** only for the O, N and C atoms because these atoms present the higher variations. The variations in the charges for C1b and C1c can be easily seen in **Figures S1** and **S2**, respectively where both figures show that the Mulliken and NPA charges present practically the same behaviours in both media. However, the behaviours of MK charges in the two forms and in both media are different from other ones. Analysing first the three charges on C1, obviously the lower values are observed on the O1 and N2 atoms in the two media but the MK charges show on practically all atoms less negative values (with exception of C12 atoms in both media) than the other ones while the NPA charges present the most negative values, with exception of C3 atoms in the two media.

The evaluation of all charges on the atoms corresponding to the C1c form show different behaviours in both media, especially in the MK charges on the C3 atoms. Hence, the changes of orientation of OH group generate notable increase on the magnitude and sign of C3 atoms in both media. In C1c, the signs of MK charges on C3 atoms are positive in both media while in C1b present negative signs.

If now the molecular electrostatic potentials (MEP) [55] on all atoms of both forms are evaluated from Table 5 we observed practically the same variations for C1b and C1c, where the most negative values are observed on the O atoms, as expected because these atoms are the most electronegative than the other ones. Thus, the following tendency it is observed in the MEP values: O > N > C > H where clearly, the H31 atoms belong to OH groups of both forms present the less negative values and, for these reasons, they are the most labile than the other ones. Analyzing the MEP mapped surfaces of C1b and C1c in gas phase from **Figure S3** we can easily observe the different colorations on these surfaces. Hence, the strong red colours are regions indicative of nucleophilic sites; the blue colours correspond to electrophilic sites while the green colours indicate clearly inert o neutral regions.

Finally, from Table S1 the bond orders (BO) expressed as Wiberg indexes by using the NBO program [52] were analysed for both C1b and C1c forms of lupinine in the two media. Observing the values from Table S1 we can see only differences in the BO values for the O, N and H atoms while for all C atoms the values remain practically constants. As evidenced by MEP values, the H31 atoms belong to OH groups of C1b and C1c show the lower values (0.779-0.778 a.u.) and, obviously, they are the most labile.

Natural Bond Orbital (NBO) study

The main donor-acceptor energy interactions were calculated for the two forms of lupinine C1b and C1c in both media by using the B3LYP/6-31G* level of theory which are presented in **Table 5**.

The results for both forms show only $\sigma \rightarrow \sigma^*$ and $n \rightarrow \sigma^*$ interactions. In the $\sigma \rightarrow \sigma^*$ interactions are involved transitions from bonding O-H and C-H orbitals toward different anti-bonding C-C, O-C, N-C, C-H orbitals while in the $n \rightarrow \sigma^*$ interactions the transitions go from lone pairs of O1 and N2 atoms toward anti-bonding C-C, C-H and O-H orbitals, as in Table 6 is detailed. Due to the different positions of OH groups in C1 and in C2, the following $\sigma C4\text{-}H14 \rightarrow \sigma^* C12\text{-}H30$, $\sigma C7\text{-}H20 \rightarrow \sigma^* C9\text{-}H23$, $\sigma C12\text{-}H29 \rightarrow \sigma^* C4\text{-}C6$ and $LP(2)O1 \rightarrow \sigma^* C12\text{-}H29$ transitions are only observed in C1 while the transitions $\sigma C4\text{-}H14 \rightarrow \sigma^* O1\text{-}C12$, $\sigma C12\text{-}H29 \rightarrow \sigma^* C3\text{-}C4$, $\sigma C12\text{-}H30 \rightarrow \sigma^* C4\text{-}C6$, $LP(1)O1 \rightarrow \sigma^* C4\text{-}C12$ and $LP(1)N2 \rightarrow \sigma^* O1\text{-}H31$ only are observed in C1c. Therefore, the total energy values evidence clearly higher stabilities for C1c in both media than C1b. Besides, C1c present higher stability in solution than in gas phase. Evidently, the position of OH group for C1b in solution could probably change to that observed in C1c.

Atoms in Molecules (AIM) studies

With the Bader's theory of Atoms in Molecules (AIM) it is possible to predict different inter or intra-molecular, ionic, covalent or H bonds interactions calculating the topological properties in the bond critical point (BCPs) or ring critical points (RCPs) [53] with the AIM2000 program [54]. These parameters are: the electron density, $\rho(r)$, the Laplacian values, $\nabla^2\rho(r)$, the eigenvalues $(\lambda 1, \lambda 2, \lambda 3)$ of the Hessian matrix and, the $|\lambda 1|/\lambda 3$ ratio by using the B3LYP/6-31G* method. Later, if $\lambda 1/\lambda 3 < 1$ and $\nabla^2\rho(r) > 0$, the interaction is clearly ionic or highly polar covalent (closed-shell interaction). Hence, in **Table S2** are presented the topological properties for the C1b and C1c forms of (-)-lupinine in both media. **Figure S4** shows the molecular graphics for C1b and C1c in gas phase with the geometry of all their BCPs and RCPs by using the B3LYP/6-31G* method. Thus, C1b presents a hydrogen H29---H15 bond interaction in both media and, as a consequence a new RCP it is observed (RCPN1). On the contrary, in C1c due to the particular position of OH group in this conformation, three new H bonds interactions are observed in gas phase (H23---O1, H31---N2 and H30---H15) while in solution the H30---H15 bonds disappear. Analysing deeply the values from Table S2, the absence of the H30---H15 bonds interaction in solution is clearly justified by the low value of density in the BCP in gas phase. For C1c, the density of the H31---N2 interaction increases in solution because decreases the distance between both involved atoms from 2.166 Å in gas phase to 1.931 Å in solution. This AIM analyses for both stable forms of (-)-lupinine show the higher stability of C1c due to the three and two new H bonds interactions, in gas phase and in aqueous solution, respectively, as compared with C1b. These results are in agreement with those observed by NBO studies.

Frontier orbitals and quantum global descriptors studies

The predictions of reactivities for the C1b and C1c conformations of (-)-lupinine in both media are very important taking into account that both species presents properties characteristics of alkaloids. Thus, the gap values were calculated from their frontier orbitals, as originally was proposed by Parr and Pearson [56]. After that, with the gap values and by using known equations the chemical potential (μ), electronegativity (χ), global hardness (η), global softness (S), global electrophilicity index (ω) and global nucleophilicity index (E) descriptors were computed by using the hybrid B3LYP/6-31G* level of theory in order to predict the behaviours of those two forms of (-)-lupinine in both media [3-9,41-45]. Thus, in **Table S3** are presented the gap and descriptors values for both stable forms of (-)-lupinine in the two media together with the corresponding equations.

Table 5. Main delocalization energies (in kJ/mol) for the most stable forms C1b and C1c of (-)-lupinine in gas phase and in aqueous solution by using B3LYP/6-31G* calculations.

Delocalization	B3LYP/6-31G*[a]			
	C1b		C1c	
	Gas	Water	Gas	Water
*σO1-H31→ σ*C4-C12*	11.95	11.62		
*σ C3-H13→σ*C4-C12*	14.71	15.97	13.59	13.63
*σ C3-H13→σ*C5-H15*	12.00	12.21	11.24	11.20
*σ C4-H14→σ*O1-C12*			18.89	19.10
*σ C4-H14→σ*N2-C3*	17.31	19.10	17.39	17.72
*σ C4-H14→σ*C6-C9*	13.17	13.04	13.50	13.63
*σ C4-H14→σ*C12-H30*	11.41	12.67		
*σ C5-H15→σ*C10-H26*	11.66	11.41	11.62	11.54
*σ C5-H16→σ*N2-C3*	16.85	16.85	17.64	17.89
*σ C5-H16→σ*C10-C11*	11.66	11.79	11.75	11.83
*σ C6-H17→σ*C4-C12*	14.46	14.09	14.17	14.30
*σ C6-H17→σ*C9-C23*	11.91	12.16		11.33
*σ C6-H18→σ*C3-C4*	12.58	12.37	12.83	12.92
*σ C6-H18→σ*C7-C9*	12.33	12.29	12.29	12.25
*σ C7-H19→σ*N2-C3*	14.67	14.13	14.34	13.88
*σ C7-H19→σ*C6-C9*	12.46	12.58	12.46	12.54
*σ C7-H20→σ*C9-H23*	11.45	11.70		
*σ C8-H21→σ*C11-H28*	11.66	11.87	11.45	11.54
*σ C8-H22→σ*N2-C3*	14.84	14.00	14.88	14.13
*σ C8-H22→σ*C10-C11*	12.67	12.79	12.58	12.58
*σ C9-H23→σ*C7-H20*	11.29	11.41	11.58	11.58
*σ C9-H24→σ*N2-C7*	17.22	17.39	17.89	18.14
*σ C9-H24→σ*C4-C6*	13.00	13.13	13.08	13.25
*σ C10-H25→σ*C3-C5*	13.38	13.21	13.67	13.63
*σ C10-H25→σ*C8-C11*	12.04	12.16	12.21	12.25
*σ C10-H26→σ*C11-H28*	11.33	11.29	11.33	11.37
*σ C11-H27→σ*N2-C8*	17.01	17.64	17.68	18.18
*σ C11-H27→σ*C5-C10*	11.70	11.83	11.70	11.83
*σ C11-H28→σ*C8-H21*	11.41	11.24	11.54	11.54
*σ C11-H28→σ*C10-H26*	11.37	11.62	11.29	11.20
*σ C12-H29→σ*C3-C4*			15.30	15.13
*σ C12-H29→σ*C4-C6*	13.08	15.97		
*σ C12-H30→σ*C4-C6*			13.71	13.75
$\Delta E_{\sigma\rightarrow\sigma^*}$	**392.58**	**399.53**	**381.59**	**393.84**
*LP(1)O1→σ*C4-C12*			15.68	15.26
*LP(2)O1→σ*C12-H29*	24.83	24.49		
*LP(2)O1→ σ*C12-H30*	22.61	19.06	35.74	32.48
*LP(1)N2→ σ*O1-H31*			48.99	58.23
*LP(1)N2→ σ*C3-H13*	30.22	28.38	25.67	23.83
*LP(1)N2→ σ*C7-H20*	30.76	29.71	26.46	25.29
*LP(1)N2→ σ*C8-H21*	31.22	29.42	27.80	25.92
$\Delta E_{LP\rightarrow\sigma^*}$	**139.64**	**131.06**	**180.33**	**180.99**
ΔE_{TOTAL}	**532.22**	**530.59**	**561.92**	**574.83**

[a]This work

The calculated gap values for the two forms of (-)-lupinine were compared with values reported for free base species of alkaloids and antihistaminic species in **Table S4** [5-7,9-14]. The high gap values for C1b and C1c of (-)-lupinine, as compared with the other species, suggest the low reactivities of both forms of lupinine than the other species. Evidently, the S(-)- form of promethazine is the most reactive in the two media. Thus, Table S4 shows that all free base species have lower gap values than those observed for C1b and C1c of (-)-lupinine.

Vibrational study

So far, the experimental infrared spectrum of lupinine is only available in the higher wavenumbers region, thus, Skolik et al [18] have studied and published this spectrum from 2840 to 2600 cm^{-1} while Omeje et al [27] have reported and asigned for lupinine only four bands located at 3419 (br, s OH), 3389 (CH_2-NCH_2), 2820 (NCH_2 stretching) and 1406 cm^{-1} (-CH_2-). Here, **Figures 3** and **4** show the comparisons between the predicted spectra for C1b and C1c of (-)-lupinine with the corresponding experimental taken from Skolik et al [18] in different regions while in **Figures 5** and **6** are presented only the predicted IR and Raman spectra for C1b and C1c in the 4000-0 cm^{-1} region. In this study, both C1b and C1c conformers were considered because the difference in energy between both forms in notably reduced from 20.20 kJ/mol in gas phase to 10.49 kJ/mol in solution. Both structures of (-)-lupinine were optimized with C_1 symmetries and are expected 87 normal vibration modes for each form. All modes are active in both spectra. The presence of various bands in the different regions observed in experimental IR spectra of Figures 3 and 4 suggests probably the presence of both forms of (-)-lupinine in the solid phase.

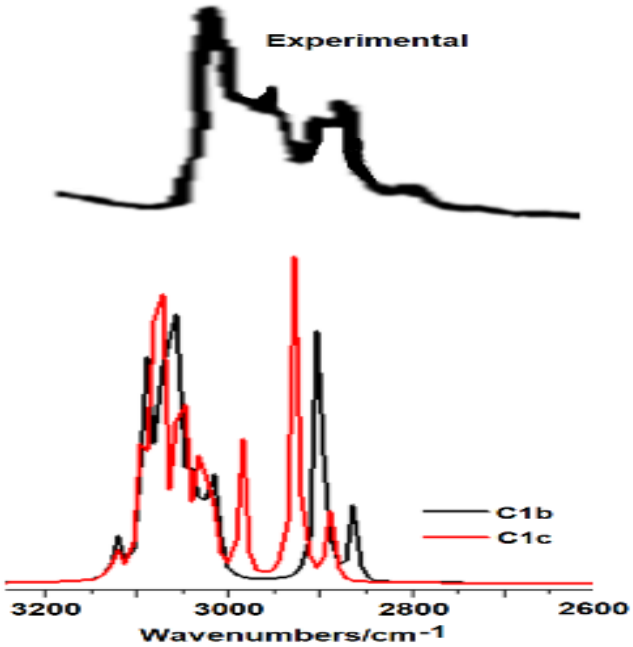

Figure 3: Experimental infrared spectrum of lupinine in the solid phase taken from Ref [18] compared with the predicted for C1b and C1c structures of (-)-Lupinine in gas phase in the 3200-2600 cm^{-1} region by using the hybrid B3LYP/6-31G* method

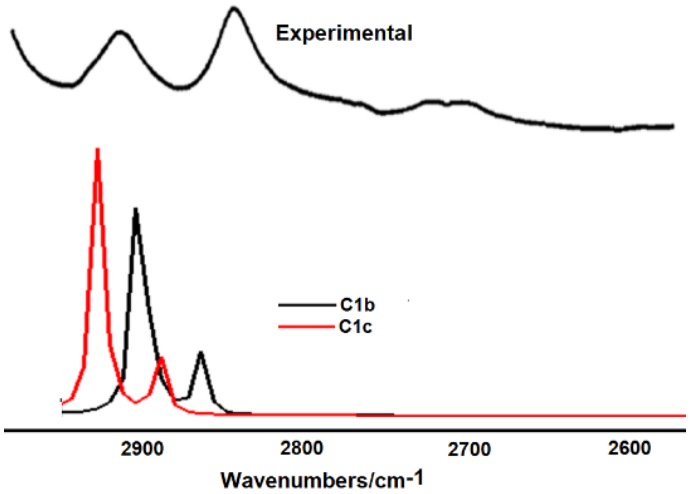

Figure 4: Experimental infrared spectrum of lupinine in the solid phase taken from Ref [27] compared with the predicted infrared spectrum for C1b and C1c structures of (-)-Lupinine in gas phase in the 3200-2600 cm^{-1} region by using the hybrid B3LYP/6-31G* method.

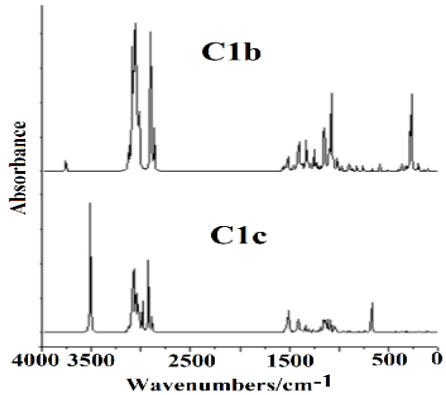

Figure 5: Predicted infrared spectrum for C1b and C1c structures of (-)-Lupinine in gas phase by using the hybrid B3LYP/6-31G* method.

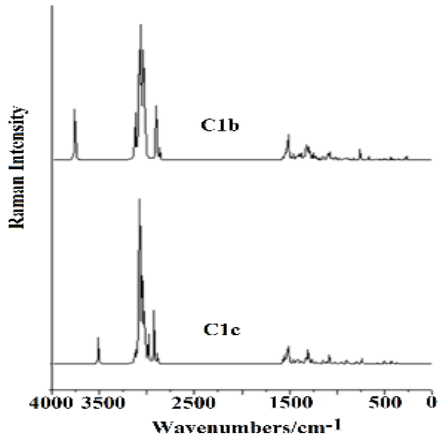

Figure 6: Predicted Raman spectrum for C1b and C1c structures of (-)-Lupinine in gas phase by using the hybrid B3LYP/6-31G* method.

On the other hand, in Figure 5 it is observed differences between the intensities of two bands predicted by calculations for both forms and those observed from the experimental spectra. Obviously, such differences could be attributed to the calculations because in gas phase are not considered the crystalline packing forces observed in the solid state. The SQMFF methodology and the Molvib program were employed to calculate the harmonic force fields of C1b and C1c at the same level of theory by using transferable scale factors and the corresponding normal internal coordinates [38-40]. Hence, with the scaled force fields and potential energy distribution (PED) contributions higher or equal to 10% the complete vibrational assignments were performed for both forms of (-)-lupinine. The observed and calculated wavenumbers and assignments for the two species of lupinine in gas phase and in aqueous solution are summarized in **Table 6**. Here, Table 6 shows clearly the differences in the assignments for both forms of (-)-lupinine and, also in the two media studied. Then, some most important assignments are discussed below.

Table 6. Observed and calculated wavenumbers (cm^{-1}) and assignments for the most stable forms C1b and C1c of (-)-lupinine in gas phase and in aqueous solution.

B3LYP/6-31G* Method[a]								
Exp.	GasC1b		GasC1c		WaterC1b		WaterC1c	
IR[c]	SQM[b]	Assignments[a]	SQM[b]	Assignments[a]	SQM[b]	Assignments[a]	SQM[b]	Assignments[a]
3419	3602	νO1-H31	3367	νO1-H31	3591	νO1-H31	3262	νO1-H31
	2993	$\nu_a CH_2$(C6)	2993	$\nu_a CH_2$(C9)	2970	$\nu_a CH_2$(C6)	2979	$\nu_a CH_2$(C9)
	2964	$\nu_a CH_2$(C5)	2969	$\nu_a CH_2$(C5)	2963	$\nu_a CH_2$(C5)	2965	$\nu_a CH_2$(C5)
	2961	$\nu_a CH_2$(C9)	2959	$\nu_a CH_2$(C11)	2959	$\nu_a CH_2$(C9)	2959	$\nu_a CH_2$(C11)
	2956	$\nu_a CH_2$(C11)	2952	$\nu_a CH_2$(C10)	2956	$\nu_a CH_2$(C11)	2958	$\nu_a CH_2$(C8)
	2947	$\nu_a CH_2$(C10)	2949	$\nu_a CH_2$(C8)	2951	$\nu_a CH_2$(C8)	2955	$\nu_a CH_2$(C7)
	2940	$\nu_a CH_2$(C8)	2945	$\nu_a CH_2$(C6)	2950	$\nu_a CH_2$(C12)	2952	$\nu_a CH_2$(C10)

	2935	$\nu_a CH_2$(C7)	2944	$\nu_a CH_2$(C7)	2947	$\nu_a CH_2$(C10)	2946	$\nu_a CH_2$(C6)
	2930	$\nu_a CH_2$(C12)	2930	$\nu_s CH_2$(C9)	2945	$\nu_a CH_2$(C7)	2934	$\nu_s CH_2$(C12)
	2922	$\nu_s CH_2$(C9)	2925	$\nu_a CH_2$(C12)	2924	$\nu_s CH_2$(C9)	2932	$\nu_s CH_2$(C9)
	2917	$\nu_s CH_2$(C5)	2924	$\nu_s CH_2$(C5)	2921	$\nu_s CH_2$(C5)	2925	$\nu_s CH_2$(C5)
	2914	$\nu_s CH_2$(C11)	2917	$\nu_s CH_2$(C11)	2916	$\nu_s CH_2$(C6)	2918	νC4-H14
	2911	$\nu_s CH_2$(C6)	2903	$\nu_s CH_2$(C10)	2915	$\nu_s CH_2$(C11)	2917	$\nu_s CH_2$(C11)
	2902	$\nu_s CH_2$(C10)	2903	νC4-H14	2915	$\nu_s CH_2$(C12)	2907	$\nu_s CH_2$(C10)
	2899	νC4-H14	2890	$\nu_s CH_2$(C6)	2904	$\nu_s CH_2$(C10)	2903	$\nu_s CH_2$(C6)
	2889	$\nu_s CH_2$(C12)	2861	$\nu_s CH_2$(C12)	2900	νC4-H14	2892	$\nu_s CH_2$(C12)
2820	2781	$\nu_s CH_2$(C8)	2806	$\nu_s CH_2$(C8)	2800	$\nu_s CH_2$(C8)	2827	$\nu_s CH_2$(C8)
	2770	$\nu_s CH_2$(C7)	2797	$\nu_s CH_2$(C7)	2796	$\nu_s CH_2$(C7)	2824	$\nu_s CH_2$(C7)
	2745	νC3-H13	2769	νC3-H13	2767	νC3-H13	2801	νC3-H13
	1493	δCH_2(C12)	1490	δCH_2(C12)	1479	δCH_2(C12)	1480	δCH_2(C12)
		δCH_2(C8)						δCH_2(C8)
	1475	δCH_2(C7)	1474	δCH_2(C7)	1466	δCH_2(C7)	1462	
		δCH_2(C6)						$wagCH_2$(C12)
	1463	δCH_2(C7)	1464	δCH_2(C6)	1453	δCH_2(C8)	1454	δO1-H31
		δCH_2(C10)		δCH_2(C10)		$wagCH_2$(C12)		δCH_2(C11)
	1459	δCH_2(C6)	1461		1450		1449	
		δCH_2(C8)						δCH_2(C7)
	1452	δCH_2(C5)	1452	δCH_2(C8)	1444	δCH_2(C8)	1445	
	1448	δCH_2(C10)	1450	δCH_2(C11)	1438	δCH_2(C6)	1439	δCH_2(C6)
		δCH_2(C9)				δCH_2(C10)		δCH_2(C10)
	1446	δCH_2(C6)	1446	δCH_2(C9)	1436	δCH_2(C11)	1437	
		δCH_2(C11)						δCH_2(C5)
	1439	δCH_2(C5)	1445	$wagCH_2$(C12)	1433	δCH_2(C9)	1431	
	1435	$wagCH_2$(C12)	1440	δCH_2(C5)	1430	δCH_2(C5)	1430	δCH_2(C9)
		$wagCH_2$(C7)						$wagCH_2$(C7)
	1424	$wagCH_2$(C8)	1424	$wagCH_2$(C8)	1421	$wagCH_2$(C7)	1417	
	1395	$wagCH_2$(C5)	1397	$wagCH_2$(C5)	1393	$wagCH_2$(C5)	1393	$wagCH_2$(C5)
		$wagCH_2$(C7)						$wagCH_2$(C9)
	1386	$wagCH_2$(C6)	1392	$wagCH_2$(C9)	1385	$wagCH_2$(C8)	1384	ρ'C4-H14
		$wagCH_2$(C8)		$wagCH_2$(C7)		$wagCH_2$(C9)		$wagCH_2$(C8)
	1379	$wagCH_2$(C7)	1383		1380		1381	
				δO1-H31				$wagCH_2$(C6)
	1372	$wagCH_2$(C11)	1378	$wagCH_2$(C6)	1371	$wagCH_2$(C11)	1373	
		$wagCH_2$(C10)				$wagCH_2$(C9)		$wagCH_2$(C11)
	1370	$wagCH_2$(C9)	1375	$wagCH_2$(C11)	1366	ρ'C3-H13	1372	
				$wagCH_2$(C10)				$wagCH_2$(C9)
				$wagCH_2$(C9)				
	1361	$wagCH_2$(C6)	1368	ρ'C3-H13	1358	$wagCH_2$(C6)	1361	
	1356	ρ'C3-H13	1361	$wagCH_2$(C10)	1356	$wagCH_2$(C10)	1357	$wagCH_2$(C10)
	1347	ρ'C4-H14	1354	ρ'C3-H13	1341	ρ'C4-H14	1350	ρC3-H13
				ρC3-H13				ρC4-H14
		ρC4-H14		ρC4-H14		ρC4-H14		
	1325	νC3-C4	1338	νC3-C4	1321	νC3-C4	1332	
	1312	ρC3-H13	1331	ρCH_2(C6)	1307	ρC3-H13	1327	ρ'C3-H13
	1291	ρCH_2(C7)	1297	ρCH_2(C8)	1288	ρCH_2(C7)	1291	ρCH_2(C8)
		ρCH_2(C5)						ρCH_2(C5)
		ρCH_2(C11)						ρCH_2(C7)
	1282	ρCH_2(C8)	1286	ρCH_2(C5)	1277	ρCH_2(C8)	1278	
		ρCH_2(C8)						ρ'C4-H14
	1261	ρCH_2(C7)	1271	ρ'C4-H14	1258	ρCH_2(C5)	1266	
		ρCH_2(C10)						ρCH_2(C8)
	1258	ρCH_2(C6)	1263	ρCH_2(C8)	1249	ρCH_2(C6)	1258	ρCH_2(C11)
	1237	ρCH_2(C12)	1253	ρCH_2(C6)	1238	ρCH_2(C12)	1246	ρCH_2(C6)
	1200	δO1-H31	1217	ρCH_2(C12)	1197	δO1-H31	1218	ρCH_2(C12)
						ρCH_2(C9)		ρCH_2(C9)
	1187	ρCH_2(C9)	1199	ρCH_2(C9)	1181	ρCH_2(C11)	1184	
				ρCH_2(C11)				ρCH_2(C11)
	1176	ρCH_2(C6)	1178	ρCH_2(C7)	1172	ρCH_2(C6)	1173	
	1173	ρCH_2(C10)	1174	ρCH_2(C10)	1168	ρCH_2(C10)	1168	ρCH_2(C10)
	1111	νN2-C7	1109	νN2-C7	1105	νN2-C7	1101	δC4C3C5
	1104	νN2-C8	1105	νN2-C8	1099	νN2-C7	1096	νN2-C7
								νN2-C8
	1089	νN2-C8	1089	νN2-C8	1085	νN2-C8	1080	νC8-C11
	1071	νC4-C6	1070	νC4-C6	1070	νC3-C5	1067	νC3-C4

	νC5-C10		νC3-C5		νC5-C10		νC3-C5
1063	νC3-C5	1067		1058		1059	
1053	νC3-N2	1048	νC3-N2	1043	νC3-N2	1035	νC3-N2
1039	νO1-C12	1035	νO1-C12	1025	νC9-C7	1027	νO1-C12
1021	νO1-C12	1017	νC9-C7	1014	νC4-C12	1016	νC9-C7
1009	νC9-C7	994	νO1-C12	1001	νO1-C12	983	νC5-C10
987	βR_1(A1)	984	βR_1(A1)	982	τwCH_2(C7)	979	νO1-C12
972	νC3-C5	964	τwCH_2(C9)	966	νC3-C5	958	τwCH_2(C9)
	τwCH_2(C9)		τwCH_2(C12)		τwCH_2(C9)		τwCH_2(C12)
939	τwCH_2(C7)	918	νC5-C10	936		916	
	τwCH_2(C12)				τwCH_2(C12)		τwCH_2(C12)
923	νC8-C11	903	τwCH_2(C12)	921	νC8-C11	902	
873	νC6-C9	891	τwCH_2(C8)	871	νC6-C9	885	τwCH_2(C8)
			νC10-C11		τwCH_2(C5)		νC6-C9
855	τwCH_2(C5)	859	νC6-C9	851		857	
	νC10-C11				νC10-C11		νC10-C11
840	τwCH_2(C8)	834	νC8-C11	841	τwCH_2(C8)	835	
	τwCH_2(C6)		τwCH_2(C6)		τwCH_2(C6)		τwCH_2(C6)
812	τwCH_2(C7)	817	τwCH_2(C7)	811	τwCH_2(C7)	814	τwCH_2(C7)
	τwCH_2(C10)						τwCH_2(C10)
800	νC4-C6	805	τwCH_2(C10)	801	τwCH_2(C10)	805	
			τwCH_2(C11)				τwCH_2(C11)
778	τwCH_2(C11)	771	τwCH_2(C9)	777	τwCH_2(C11)	770	
	τwCH_2(C5)						νC4-C12 νC4-C6
767	νC4-C12	756	νC4-C12	767	νC4-C6	756	
	νC3-N2		τwCH_2(C5)		νC3-N2		δC3C4C12
714	τwCH_2(C5)	745		718		745	τwCH_2(C5)
639	δC3C4C12	705	νC3-N2	656	δC3C4C12	701	νC3-N2
	τwCH_2(C9)						τO1-H31
562	δC6C4C12	598	τO1-H31	551	βR_1(A1)	579	
528	βR_1(A2)	538	βR_1(A1)	539	βR_1(A2)	530	βR_1(A1)
487	βR_3(A2)	527	βR_1(A2)	480	δC6C4C12	526	βR_1(A2)
468	βR_2(A2)	482	βR_2(A2)	472	βR_2(A2)	480	βR_2(A2) τR_2(A2)
			βR_2(A2)				βR_2(A2)
421	βR_2(A1)	453	δC6C4C12	421	βR_3(A2)	453	
			βR_3(A2)				βR_3(A1)
382	βR_3(A1)	424	βR_3(A1)	380	βR_2(A1)	425	
			βR_2(A1)		τR_1(A1)		βR_2(A1)
350	τR_1(A1)	408		353		408	δC4C12O1
							τR_1(A1)
346	τR_1(A2)	368	τR_1(A1)	347	τR_1(A2)	370	δC6C4C12
	δC4C3C5						βR_3(A2)
311	δC4C12O1	353	τR_2(A1)	316	βR_3(A1)	348	
					δC4C12O1		τR_1(A2)
308	τR_2(A1)	329	τR_1(A2)	302	δC4C3C5	335	
267	τR_3(A1)	307	τR_3(A1)	272	τR_3(A1)	307	τR_3(A1)
241	τO1-H31	274	δC4C3C5	240	τO1-H31	269	τR_1(A1)
	δC3C4C12		δC3C4C12				τR_3(A2)
207	τR_2(A2)	240	δC4C12O1	214	δC3C4C12	235	
185	τR_3(A2)	180	τR_3(A2)	185	τR_3(A2)	187	τR_3(A2)
	τR_2(A1)						τR_2(A1)
124	τR_3(A2)	148	τ_wO1-C12	140	τR_2(A1)	148	
89	τR_2(A2)	105	τR_2(A2)	84	τ_wO1-C12	105	τR_2(A2)
56	τ_wO1-C12	92	τO1-H31	78	τR_2(A2)	99	τ_wO1-C12

Abbreviations: ν, stretching; β, deformation in the plane; γ, deformation out of plane; wag, wagging; τ , torsion; β_R, deformation ring τ_R, torsion ring; ρ, rocking; τw, twisting; δ, deformation; a, antisymmetric; s, symmetric; (A_1), Ring 1; (A_2), Ring 2. [a]This work, [b]From scaled quantum mechanics force field, [c]From Ref [27], [d]From Ref [13].

Assignments.

4000-2500 cm^{-1} region. This region is typical of stretching modes corresponding to the OH, C-H and CH_2 groups of C1b and C1c, as assigned in other species with similar groups [3-9,41-45,61-63]. All these modes are assigned as predicted the theoretical calculations and, as reported in the literature for compound with similar groups [3-9,41-45,61-63]. For C1b and C1c, there is two aliphatic C3-H13 and C4-H14 groups where, this latter group belong to chiral C4 atom which is predicted in gas phase C1b at 2899 cm^{-1} and, in C1c, at 2900 cm^{-1}. In solution, these modes for C1b and C1c are shifted at 2903 and 2918 cm^{-1}, respectively. The other C3-H13 stretching mode

are predicted 2801 and 2747 cm^{-1}, hence, these can be assigned to the broad IR band at 2820 cm^{-1}. The two antisymmetrical and symmetric stretching modes expected for C1b and C1c are predicted by SQM calculations between 2993 and 2770 cm^{-1}, therefore, the broad IR band at 2820 cm^{-1} can be also assigned to these vibration modes. The symmetry of these modes cannot be defined because the experimental Raman was not published yet but, we know that the most intense bands in this spectrum should be assigned to symmetric modes.

1500-1000 cm^{-1} region. In this region are expected the C-O, C-N and C-C stretching modes, deformation, rocking and waging modes of CH_2 groups and, also the OH deformation and C-H rocking modes of both forms [3-9,41-45,61-63]. Hence, from 1493 to 1430 cm^{-1} can be assigned to the CH_2 deformation modes while IR bands in the 1454/1356 and 1331/1168 cm^{-1} regions can be assigned to waging and rocking modes of these groups, respectively. The two C-H rocking modes are predicted between 1384 and 1266 cm^{-1} while the OH deformations in gas phase and in solution are predicted at 1200/1197 and 1454/1378 cm^{-1}, respectively. On the other hand, the C-O, C-N and C-C stretching modes can be assigned from 1111 up to 701 cm^{-1}.

1000-56 cm^{-1} region. The CH_2 twisting modes are predicted in this region together with the OH torsion modes, C-C-C, C-C-O deformations rocking, deformation and torsion modes of both rings and other skeletal modes detailed in Table 6. Hence, all these modes can be assigned as predicted by SQM calculations modes and, as reported for species containing similar groups [3-9,41-45,61-63].

Force Fields

The harmonic force fields for C1b and C1c of (-)-lupinine in both media were employed to calculate the corresponding scaled force constants with the B3LYP/6-31G* method because these factors are useful to predict the features of different bonds. As detailed in section computational details, the harmonic force fields were computed with the SQMFF methodology [38] and the Molvib program [40]. Thus, in **Table 7** are summarized the scaled force constants for C1b and C1c in both media. In general, in both conformations are observed the same force constants values, however, notable differences are observed in the force constants related to the C-OH groups, as expected because the positions of these groups are the differences between both conformers. Thus, both *f(νC-O)* and *f(νO-H)* force constants present different values in gas phase and in solution. The *f(νC-O)* force constant for C1c is higher than the corresponding to C1b in gas phase while in this same medium the *f(νO-H)* force constant of C1b is slightly higher than the corresponding to C1c. In solution, the same relation is obtained having the *f(νC-O)* force constant of C1c higher value than the corresponding to C1b while the *f(νO-H)* force constant of C1b is higher than the corresponding to C1c. On the other hand, the *f(δCH_2)* force constants for both species are different in a same medium but they have approximately the same values in solution, as observed in Table 7.

Table 7. Scaled internal force constants for both C1b and C1c forms of (-)-lupinine in different media by using the B3LYP/6-31G* method.

Force constant	Lupinine			
	Gas phase		Aqueous solution	
	C1b	C1c	C1b	C1c
f(νC-H)	4.42	4.43	4.44	4.51
f(νC-O)	4.87	5.09	4.61	4.73
f(νO-H)	7.25	6.32	7.21	5.92
f(νC-C)	4.03	4.02	4.04	4.05
f(νC-N)	4.80	4.31	4.33	4.18
f(νCH_2)	4.68	4.69	4.70	4.71
f(δCH_2)	0.85	0.75	0.84	0.74

Units are mdyn $Å^{-1}$ for stretching and mdyn Å rad^{-2} for angle deformations
[a]This work

NMR study

The ^{1}H and ^{13}C NMR chemical shifts for all forms of (+) and (-)-lupinine were predicted in aqueous solution, benzene and $CDCl_3$ by using the GIAO [41] and the B3LYP/6-31G* methods while the experimental available were taken from Ref [19-21,23,64,65]. Observed and calculated ^{1}H chemical shifts can be seen from **Tables S5** to **S8** together with the comparisons among experimental and theoretical values expressed by means of the RMSD values. Table S5 shows reasonable correlations for the hydrogen nucleus of both C0 and C1a forms, especially with values between 0.44 and 0.47 ppm while better correlations were found for the most stable C1b and C1c forms of (-)-lupinine from Table S6, with values between 0.54 and 0.22 ppm. On the other hand, when

the C nucleus for all (+) and (-)-lupinine forms are compared from Tables S7 and S8 the RMSD values increase to 8.8 and 7.0 ppm. Thus, the better concordances are observed for the C1c form in gas phase and in aqueous solution, as shown in Tables S7 and S8. Note that the chemical shifts for the H31 atoms belonging to OH groups of C1b and C1c were not included in Tables S5 and S6 because the values were predicted with negative signs indicating probably that these atoms are involved in H bonds interactions. Evidently, the slight differences in the results can be rapidly attributed to the 6-31G* basis set different from that recommended 6-311++G** basis set.

Electronic spectra

The ultraviolet-visible spectra for all (+) and (-)-lupinine forms of lupinine were predicted in methanol solution by using the B3LYP/6-31G* method and they are compared in **Figure S5.** In Table S9 are presented the positions and intensities of only two bands observed in each spectrum compared with the experimental bands reported for lupinine in methanol solution by Anderson and Steckler and Omeje et al from Ref [17,22]. The predicted UV-Vis spectra evidence the presence of all forms of lupinine including the most stable C1c form of (-)-lupinine despite in this latter form the amine is forming an intra-molecular H bond while the amine groups are free in the other ones. The two bands predicted by calculations and experimentally observed in the experimental spectrum, are associated to transitions $\sigma \rightarrow \sigma^*$, $n(O) \rightarrow \sigma^*$ and $n(N) \rightarrow \sigma^*$, as supported by NBO analysis.

Electronic Circular Dichroism (ECD)

The ECD spectra of all (+) and (-)-lupinine forms in methanol solution were predicted by using the B3LYP/6-31G* method and they are compared in **Figure 7**. The graphic representations were performed by using the software *GaussSum* [66]. four theoretical spectra show two bands in the 100-300 nm in different positions, hence, in C0 the two bands are observed in 197 and 208 nm where the first present a negative Cotton effect and the other one is positive, in C1b both present negative Cotton effect and are observed in 202 and 228 nm while in C1b is observed one band negative in 207 nm. In C1c, the two bands present negative Cotton effect in 200 and 209 nm. Hence, only the C1b form presents in methanol solution similar to experimental ECD spectrum reported by Ishave et al [35]. Hence, in a methanol solution clearly is present the C1b form of (-)-lupinine probably due to that in C1c the OH group presents an intramolecular H bond.

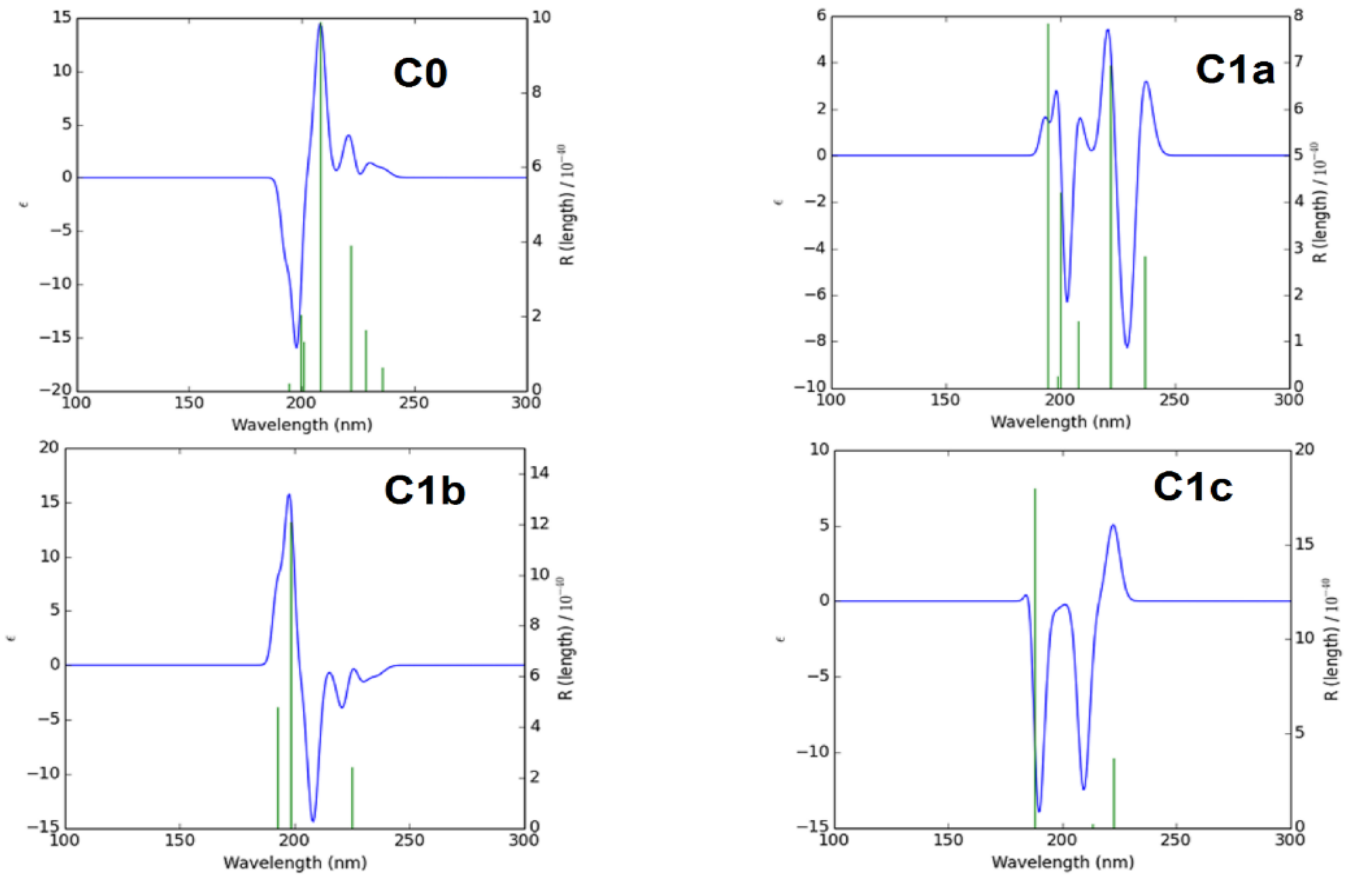

Figure 7: Comparisons between the predicted ECD spectrum for all (+) and (-) forms of lupinine in methanol solutions by using B3LYP/6-31G* level of theory.

Conclusions

In this work, four (+) and (-)- molecular structures of quinolizidine alkaloid lupinine, named C0, C1a, C1b and C1c, were theoretically determined in gas phase and in aqueous solution by using hybrid B3LYP/6-31G* calculations. This way, the C0 structure correspond to the (+) form while the C1a, C1b and C1c structures correspond to the (-)-lupinine forms. The studied structural, electronic, topological and vibrational properties have evidenced that the most stable C1c form present the higher populations in both media while the predicted infrared, Raman, ^{1}H-NMR and ^{13}C-NMR and ultra-visible spectra suggest that other forms in lower proportion probably could be present in, water, chloroform and benzene solutions, as evidenced by the low RMSD values observed in the ^{1}H- and ^{13}C-NMR chemical shifts.

The C1c form presents the lower corrected solvation energy in water while the NBO and AIM studies suggest for this form a high stability in both media.

The frontier orbitals studies reveal higher gap values for C1c form of (-)-lupinine in both media, as compared with heroin, morphine, cocaine, scopolamine and tropane alkaloids, suggesting a lower reactivity for this alkaloid.

The harmonic force fields, force constants and the complete vibrational assignments for the 87 normal vibration modes expected for the most stable C1b and C1c forms of (-)-lupinine are reported here for first time.

In addition, the predicted ECD spectra of all (+) and (-)-lupinine forms in methanol solution evidence clearly that the C1b forms is present in the solution because its spectrum presents a negative Cotton effect as observed in the experimental one.

Acknowledgements. This work was supported with grants from CIUNT Project Nº 26/D608 (Consejo de Investigaciones, Universidad Nacional de Tucumán).The authors would like to thank Prof. Tom Sundius for his permission to use MOLVIB.

References

1. V.R. Sweta, T. Lakshmi, Pharmacological profile of tropane alkaloids, *J. Chem. and Pharm Res*, 7(5) (2015) 117-119; https://doi:10.24193/subbbiol.2017.2.01
2. L. Fernández-López, M. Falcón Romero, G. Prieto-Bonete, C. Pérez-Martínez, J. Navarro-Zaragoza, D. Suarez, A. Luna Maldonado, Improving detection window of scopolamine, *Forensic Sci. Int*. 287 (2018) 10; https://doi.org/10.1016/j.forsciint.2018.04.011
3. S.A. Brandán, Why morphine is a molecule chemically powerful. Their comparison with cocaine. *Indian Journal of Applied Research*, 7(7) (2017) 511-528; https://doi.org/10.15373/2249555X
4. R. Rudyk, S.A. Brandán, Force field, internal coordinates and vibrational study of alkaloid tropane hydrochloride by using their infrared spectrum and DFT calculations. *Paripex. A Indian Journal of Research*, 6(8) (2017) 616-623; https://doi.org/10.15373/22501991
5. D. Romani, S.A. Brandán, Vibratonal analyses of alkaloid cocaine as free base, cationic and hydrochloride species based on their internal coordinates and force fields. *Paripex. A Indian Journal of Researc*h, 6(9) (2017) 587-602; https://doi.org/10.15373/2249555X
6. S.A. Brandán, Understanding the potency of heroin against to morphine and cocaine. *IJSRM*, 12(2) (2018) 97-140. https://doi.org/10.15373/22501991
7. R.A. Rudyk, M.A. Checa, K.A. Guzzetti, M.A. Iramain, S.A. Brandán, Behaviour of N-CH_3 Group in Tropane Alkaloids and correlations in their Properties. *IJSRM*, 10 (4) (2018) 70-97.
8. M.E. Manzur, R.A. Rudyk, S.A. Brandán, Evaluating properties of free base, cationic and hydrochloride Species of potent psychotropic 4-Bromo-2,5-dimethoxyphenethylamine drug, *International Journal of Current Advanced Research*, 8(3) (2019) 17166-17170; https://doi.org/10.24327/IJCAR
9. M.A. Iramain, J. Ruiz Hidalgo, S.A. Brandán, Predicting properties of species derived from N-(1H-indol-3-ylmethyl)-N,N-dimethylamine, Gramine, a indol alkaloid, *International Journal of Current Advanced Research*, 8(4) (2019) 18113-18124; https://doi.org/10.24327/IJCAR
10. S. Okuda, I. Murakoshi, H. Kamata, Y. Kashida, J. Haginiwa, K. Tsuda, Studies on Lupin Alkaloids. I. the Minor Alkaloids of Japanese Sophora flavescens. S, *Chem. Pharm. Bull*., 13 (1965) 482; https://doi.org/10.1248/cpb.13.482
11. S. Okuda, H. Kataoka, and K. Tsuda, Studies on Lupin Alkaloids. II. Absolute Configuration of Lupin Alkaloid. I, *Chem. Pharm. Bull*., 13 (1965) 487; https://doi.org/10.1248/cpb.13.487
12. S. Okuda, H. Kataoka, and K. Tsuda, Studies on Lupin Alkaloids. III. Absolute Configurations of Lupin Alkaloids. II, *Chem. Pharm. Bull*., 13 (1965) 491, https://doi.org/10.1248/cpb.13.491.

13. S. Okuda, M. Yoshimoto, and K. Tsuda, Studies on Lupin Alkaloids. IV. Total Syntheses of Optically Active Matrine and Allomatrine. *Chem. Pharm. Bull*., 14 (1966) 275; https://10.1248/cpb.14.275.
14. F. Bohlmann, D. Schumann, Chapter 5 Lupine Alkaloids, The Alkaloids: Chemistry and Physiology, Edited by R.H.F. Manske, Academic Press Inc., New York, 9, (1967) 175-221; https://doi.org/10.1002/ange.19670790329
15. Koziol A, Kosturkiewicz Z, Podkowinska H. Structure of the Alkaloid Lupinine, *Acta Cryst.* B34 (1978) 3491–3494; https://doi.org/10.1107/S0567740878011437
16. L. Marion, D. A. Ramsay, and R. Norman, The Infrared Absorption Spectra of Alkaloids, *J. Am. Chem Soc. 73*, (1951) 305–308; https://doi.org/10.1364/JOSA.23000092 .
17. A. G. Anderson Jr. and B. M. Steckler, Azulene. VIII. A Study of the Visible Absorption Spectra and Dipole Moments of Some 1- and 1,3-Substituted Azulenes *J. Am. Chem Soc.* 81(18) (1959) 4941–4946; https://doi.org/10.1021/ja01527a046
18. J. Skolik and P. J. Krueger, "Correlation Between the Stereochemistry of Quinolizidine Alkaloids and Their Infrared Spectra From 2840-2600 cm-1, *Tetrahedron*. 24 (1968) 5439–5456.
19. H. Podkowinska, NMR Spectroscopic Study of Lupinine and Epilupinine Salts and Amine Oxides, *Organic Magnetic Resonance,* 22(6) (1984) 379–384; HTTPS://10.1002/MRC.1270220607
20. W.M. Golebiewski, Assignment of the proton spectrum of lupinine by two-dimensional techniques, *Academy of Sciences Chemistry*, 34 (1986) 191–198; https://doi.org/10.1002/mrc.1260241115
21. J. Rana, D.J. Robins, Application of 13C-NMR Spectroscopy to Study the Biosynthesis of the Quinolizidine Alkaloids Lupinine and Sparteine, *J. Chem. Soc. Perkin Trans I* (1986) 1133–1137; https://doi.org/10.1039/p19860001133
22. A.M. Halpern, M.W. Legenza, Photophysics of Satured Amino Alcohols. Lupinine and Model Compounds: Excited-state Intramolecular Association, *J Phys. Chem.* 94(26) (1990) 8885–8890; 10.1016/j.saa.2013.07.047
23. D. S. Rycroft, D. J. Robins, and I. H. Sadler, Revised Assignment of the 1H-NMR Spectrum of the Quinolizidine Alkaloid Lupinine, *Magnetic Resonance in Chemistry*, 30 (1992) 15–17; https://doi.org/10.1002/MRC.1260301306
24. S. Ohmiya, K. Saito, and I. Murakoshi, Lupine alkaloids, Academic Press Inc.,vol. 47, (1995) 1–114; https://doi.org/10.1080/13880200802448674.
25. G. Polya, Biochemical Targets of Plant Bioactive Compounds, CRC Press, EEUU, ISBN 0415-30829-1 (2003).
26. P. Nana, Potential of Integrating Calpurnia aurea with Entomopathogenic Fungus Metarhizium anisopliae for the Control of Rhipicephalus appendiculatus and Rhipicephalus pulchellus Paulin Nana A thesis submitted in fulfilment for the Degree of Doctor of Philosophy. (2010).
27. E. O. Omeje et al., A novel sesquiterpene acid and an alkaloid from leaves of the Eastern Nigeria mistletoe , Loranthus micranthus with potent immunostimulatory activity on C57BL6 mice splenocytes and CD69 molecule, *Pharmaceutical Biology*, 49(12) (2011) 1271–1276; https://doi.org/10.3109/13880209.2011.621129
28. R. K. Bohn, Microwave spectroscopy newsletter LV List of Contributors I Table of Contents Contributor. *24th Austin Symposium on Molecular Structure and Dynamics at Dallas (ASMD@D)*, Dallas, Texas, USA (2012).
29. S. Grimme, A General Quantum Mechanically Derived Force Field (QMDFF) for Molecules and Condensed Phase Simulations, *Chemical Theory and Computation*, 10(10) (2014) 4497–4514; https://doi.org/10.1021/ct500573f.
30. M. Vallejo Lopez, Structural Studies of Biomolecular Building Blocks and Molecular Aggregates, Thesis Doctoral, (2014).
31. H. Hotti, The killer of Socrates exposed–Coniine in the plant kingdom The killer of Socrates plant kingdom. ISBN 978-951-38-8459-8 (2016); https://doi.org/10.3390/molecules22111962
32. S. Ravi, B. Shanmugam, G. Venkata, Identification of food preservative , stress relief compounds by GC–MS and HR-LC/Q-TOF/MS ; evaluation of antioxidant activity of Acalypha indica leaves methanolic extract (in vitro) and polyphenolic fraction (in vivo), *J. Food Sci. Technol.*, 54(6) (2017) pp. 1585–1596, https://doi.org/10.1007/s13197-017-2590-z .
33. P. C. Avendaño, Identificación y cuantificación de alcaloides de lupino. *(Lupinus mutabilis Sweet)*. VI World Congress of Quinoa, University of Turku (2017); https://doi.org/10.15446/acag .
34. R. W. Hoffman, Classical Methods in Structure Elucidation of Natural Products, Lupinine, *Wiley*, (2018) 113-120; https://doi.org/10.1002/9783906390819

35. A. I. Ishave, Kh. A. Aslanov, A. S. Sadykov, M. A. Ramazanova, An investigation of quinolizidine alkaloids by the optical rotatory dispersion (ORD) method. I. ORD of alkaloids of the lupinine, cytisine, sparteine, and aphyllinic acid group, V. I. Lenin Tashkent State University. 8(3) (1972) 322-326. https://doi.org/10.1007/BF00563740
36. A.D. Becke, Density-functional exchange-energy approximation with correct asymptotic behavior. *Phys. Rev.*, A38 (1988) 3098-3100; https://10.1103/PhysRevA.38.3098.
37. C. Lee, W. Yang, R.G. Parr, Development of the Colle-Salvetti correlation-energy formula into a functional of the electron density. *Phys. Rev*., B37 (1988) 785-789; https://doi.org/10.1103/physrevb.37.785
38. P. Pulay, G. Fogarasi, G. Pongor, J.E. Boggs, A. Vargha, Combination of theoretical ab initio and experimental information to obtain reliable harmonic force constants. Scaled quantum mechanical (QM) force fields for glyoxal, acrolein, butadiene, formaldehyde, and ethylene. *J. Am. Chem. Soc*., 105 (1983) 7073; https://doi.org/10.1021/ja00362a005
39. a) G. Rauhut, P. Pulay, Transferable Scaling Factors for Density Functional Derived Vibrational Force Fields. *J. Phys. Chem*., 99 (1995) 3093-3100; https://doi.org/10.1021/j100010a019 b) *Correction:* Rauhut G, Pulay *P. J. Phys. Chem.*, 99 (1995) 14572.
40. T. Sundius, Scaling of ab-initio force fields by MOLVIB. *Vib. Spectrosc*., 29 (2002) 89-95.
41. D. Romani, S.A. Brandán, M.J. Márquez, M.B. Márquez, Structural, topological and vibrational properties of an isothiazole derivatives series with antiviral activities. *J. Mol. Struct*., 1100 (2015) 279-289; https://doi.org/10.1016/j.molstruc.2015.07.038 .
42. H. Abdelmoulahi, H. Ghalla, S. A. Brandán, S. Nasr, Structural study and vibrational analyses of the monomeric, dimeric, trimeric and tetrameric species of acetamide by using the FT-IR and Raman spectra, DFT calculations and SQM methodology, *J. Mater. Environ. Sci*. (JMESCN) 6 (11) (2015) 3094-3109.
43. E. Romano, M.V. Castillo, J.L. Pergomet, J. Zinczuk, S.A. Brandán, Synthesis, structural and vibrational analysis of (5, 7-Dichloro-quinolin-8-yloxy) acetic acid. *J. Mol. Struct*., 1018 (2012) 149–155; https://doi.org/10.1016/j.molstruc.2012.03.013 .
44. M.A. Iramain, L. Davies, S.A. Brandán, Structural and spectroscopic differences among the Potassium 5-hydroxypentanoyltrifluoroborate salt and the furoyl and isonicotinoyl salts. *J Mol. Struct*., 1176 (2019) 718-728; https://doi.org/10.1016/j.molstruc.2018.09.015.
45. N. Issaoui, H. Ghalla, S.A. Brandán, F. Bardak, H.T. Flakus, A. Atac, B. Oujia, Experimental FTIR and FT-Raman and theoretical studies on the molecular structures of monomer and dimer of 3-thiopheneacrylic acid. *J. Mol. Struct.*, 1135 (2017) 209-221; https://doi.org/10.1016/j.molstruc.2017.01.074.
46. Nielsen AB, Holder AJ. Gauss View 3.0. User's Reference, GAUSSIAN Inc., Pittsburgh, PA, (2000–2003).
47. M.J. Frisch, G.W. Trucks, H.B. Schlegel, G.E. Scuseria, M.A. Robb, J.R. Cheeseman, G. Scalmani, V. Barone, B. Mennucci, G.A. Petersson, H. Nakatsuji, M. Caricato, X. Li, H.P. Hratchian, A.F. Izmaylov, J. Bloino, G. Zheng, J.L. Sonnenberg, M. Hada, M. Ehara, K. Toyota, R. Fukuda, J. Hasegawa, M. Ishida, T. Nakajima, Y. Honda, O. Kitao, H. Nakai, T. Vreven, J.A. Montgomery, J.E. Peralta, F. Ogliaro, M. Bearpark, J.J. Heyd, E. Brothers, K.N. Kudin, V.N. Staroverov, R. Kobayashi, J. Normand, K. Raghavachari, A. Rendell, J.C. Burant, S.S. Iyengar, J. Tomasi, M. Cossi, N. Rega, J.M. Millam, M. Klene, J.E. Knox, J.B. Cross, V. Bakken, C. Adamo, J. Jaramillo, R. Gomperts, R.E. Stratmann, O. Yazyev, A.J. Austin, R. Cammi, C. Pomelli, J.W. Ochterski, R.L. Martin, K. Morokuma, V.G. Zakrzewski, G.A. Voth, P. Salvador, J.J. Dannenberg, S. Dapprich, A.D. Daniels, O. Farkas, J.B. Foresman, J. Ortiz, J. Cioslowski, D.J. Fox, Gaussian, Inc., Wallingford CT, (2009).
48. S. Miertus, E. Scrocco, J. Tomasi. Electrostatic interaction of a solute with a continuum. *Chem. Phys*, 55 (1981) 117–129; https://doi.org/10.1016/0301-0104(81)85090-2 .
49. J. Tomasi, J. Persico, Molecular Interactions in Solution: An Overview of Methods Based on Continous Distributions of the Solvent. *Chem. Rev*., 94 (1994) 2027-2094; https://doi.org/10.1021/cr00031a013.
50. A.V. Marenich, C.J. Cramer, D.G. Truhlar, Universal solvation model based on solute electron density and a continuum model of the solvent defined by the bulk dielectric constant and atomic surface tensions. *J. Phys. Chem*., B113 (2009) 6378-6396; https://doi.org/10.1021/jp810292n
51. P. Ugliengo, Moldraw Program, University of Torino, Dipartimento Chimica IFM, Torino, Italy, (1998).
52. E. Glendening, J.K. Badenhoop, A.D. Reed, J.E. Carpenter, F. Weinhold, NBO 3.1; Theoretical Chemistry Institute, University of Wisconsin; Madison, WI, (1996).
53. R.F.W. Bader, Atoms in Molecules, A Quantum Theory, Oxford University Press, Oxford, (1990), ISBN: 0198558651.
54. F. Biegler-Köning, J. Schönbohm, D. Bayles, AIM2000; A Program to Analyze and Visualize Atoms in Molecules. *J. Comput. Chem.*, 22 (2001) 545; https://doi.org/10.1002/1096-987X(20010415)22:5<545::AID-JCC1027>3.0.CO;2-Y .

55. B.H. Besler, K.M. Merz Jr, P.A. Kollman, Atomic charges derived from semiempirical methods. *J. Comp. Chem.*, 11 (1990) 431-439; https://doi.org/10.1002/jcc540110404 .
56. R.G. Parr, R.G. Pearson, Absolute hardness: companion parameter to absolute electronegativity. *J. Am. Chem. Soc.*, 105 (1983) 7512-7516; https://doi.org/10.1021/ja00364a005
57. J-L. Brédas, Mind the gap! *Materials Horizons*, 1 (2014) 17–19; https://doi.org/10.1039/C3MH00098B
58. G. Keresztury, S. Holly, G. Besenyei, J. Varga, A.Y. Wang, J.R. Durig. Vibrational spectra of monothiocarbamates-II. IR and Raman spectra, vibrational assignment, conformational analysis and ab initio calculations of S-methyl-N, N-dimethylthiocarbamate. *Spectrochim. Acta*, 49A (1993) 2007-2026; https://doi.org/10.1016/S0584-8539(09)91012-1
59. D. Michalska, Wysokinski. The prediction of Raman spectra of platinum (II) anticancer drugs by density functional theory. *Chemical Physics Letters*, 403 (2005) 211-217; https://doi.org/10.1016/j.cplett.2004.12.096
60. R. Ditchfield, Self-consistent perturbation theory of diamagnetism. I. A gage-invariant LCAO (linear combination of atomic orbitals) method for NMR chemical shifts. *Mol Phys*, 27 (1974) 714–722; https://doi.org/10.1080/00268977400100711
61. M.E. Manzur, S.A. Brandán. S (-) and R(+) Species Derived from Antihistaminic Promethazine Agent: Structural and Vibrational Studies, Submitted to *Heliyon* (2019);. https://doi.org/10.1016/j.heliyon.2019.e02322
62. M.J. Márquez, M.A. Iramain, S.A. Brandán. *Ab-initio* and Vibrational studies on Free Base, Cationic and Hydrochloride Species Derived from Antihistaminic Cyclizine agent. *IJSRM*, 12(2) (2018) 97-140; https://doi.org/10.15373/22501991
63. R.A. Rudyk, M.A. Checa, C.A.N. Catalán, S.A. Brandán. Structural, FT-IR, FT-Raman and ECD spectroscopic studies of free base, cationic and hydrobromide species of scopolamine alkaloid. *J. Mol. Struct.*, 1180 (2019) 603-617; https://doi.org/10.1016/j.molstruc2018.12.040 .
64. A.C. Cutter, I.R. Miller, J.F. Keily, R.K. Bellingham, M.E. Light, R.C.D Brown. Total Syntheses of (-) Epilupinine and (-)-Tashiromine using Imino-Aldol Reactions. *Org. Lett*., 13(15) (2011) 3988-3991; https://doi.org/10.1021/ol2015048
65. L.S. Santos, Y. Mirabal-Gallardo, N. Shankaraiah, M.J. Simirgiotis, Short Total Synthesis of (-)-Lupinine and (-)-Epiquinamide by Double Mitsunobu Reaction. *Synthesis*, 1 (2011) 51-56; https://doi.ord/10.1055/s-0030-1258356.
66. N.M. O'Boyle, A.L. Tenderholt. K.M. Langner, GaussSum software, *J. Comp. Chem*. 29 (2008) 839-845; https://doi.org/10.1002/jcc.20823 .

(2019) ; http://www.jmaterenvironsci.com